www.sciencemag.org/content/350/6263/aab0988/suppl/DC1

Supplementary Materials for

Bidirectional Notch signaling regulates *Drosophila* intestinal stem cell multipotency

Zheng Guo and Benjamin Ohlstein*

*Corresponding author. E-mail: bo2160@columbia.edu

Published 20 November 2015, *Science* **350**, aab0988 (2015)
DOI: 10.1126/science.aab0988

This PDF file includes:

Materials and Methods

Drosophila stocks

esg-Gal4 UAS-GFP/CyO (*1*), *esg-Gal4 UAS- GFP tub-Gal^{80}/CyO* (*1*), *UAS-Dl RNAi* (Vienna *Drosophila* RNAi Center, #37288), *hsflp tubGAL80 FRT19A/FM7; tub-Gal4 UAS-GFP/TM3,Ser* (*MARCM 19A*), *FRT19A; ry506* (Bloomington *Drosophila* Stock Center [BL], #1709), *Notch^{55e11}FRT19A/FM7* (BL#28813), *yw hsflp tub-Gal4 UAS-dsRed; FRT82B tub-Gal80/TM3, Ser* (*MARCM 82B*)(*46*), *FRT82B Dl^{RevF10}/TM6B* (*3*), *UAS-Notch RNAi* (BL#7078), *UAS-Notch^{DN}* (obtained from Myriam Zecca and Gary Struhl, Columbia University Medical Center), *Gbe+ Su(H)-LacZ* (*NRE-lacZ*) (*3*), *baz^{4} FRT19A/FM7B* (obtained from Chris Doe, Institute of Neuron Science, stock 7c4), *UAS-baz RNAi* (BL#31523), *UAS-Notch^{1790}* (*24*), *UAS-Notch$^{1792-2156}$* (*24*), *UAS-Notch$^{1895-2116}$* (*24*) (obtained from Toby Lieber, Simon Kidd and Gary Struhl, Columbia University Medical Center), *yw hsflp UAS-GFP; tub-Gal80 FRT40A; tub-Gal4/ TM6B, Tb* (*MARCM 40A*) *, nub^{1} FRT40A/CyO* (obtained from Richard Mann, Columbia University Medical Center), *UAS-asense* (obtained from Hugo Bellen, Baylor College of Medicine).

Pupal ISC and Pros+ cell counting

esg-Gal4 UAS-GFP (*esg>GFP*) flies were reared at 25^{o}C during all of pupal development. When LL3 female larvae began metamorphosis, white pupae were placed into an empty vial at 25^{o}C and designated as being at 0h after pupal formation (APF). Intestines were dissected at 24, 30, 40, 43, 44, 48, 54 67, 72, 78, 91, and 96h APF followed by immunofluorescence staining.

Linage tracing pupal ISCs by MARCM clones induced at different time points of pupal development

FRT40A MARCM flies were cultured at 25°C during all of pupal development (except during heat shock induction). When LL3 female larvae began metamorphosis, white pupae were placed into an empty vial at 25°C and designated as being at 0h APF. Mosaic Analysis with a Repressible Cell Marker (MARCM) labels one of the two daughter cells after mitotic division. ISC asymmetric divisions occur between 44-56 APF. To label ISCs before their asymmetric division, MARCM clones were induced at 36h APF for 1 hour and intestines were examined at 96h APF by immunofluorescence staining. To label ISC or ee cell symmetric divisions, *FRT40A* MARCM flies were heat shocked at 48h APF for 1 hour (time when ISCs are undergoing asymmetric divisions), and were examined at 96h APF, followed by immunofluorescence staining. To trace MARCM clones after the first round of asymmetric divisions. *FRT40A* MARCM flies were heat shocked at 30h APF for 1 hour, and were examined at 56h APF, followed by immunofluorescence staining.

Knock Down of Baz during pupal development

esg^{ts}>*GFP* (control) and esg^{ts}>*GFP baz RNAi* flies were cultured at 18°C. Late Larval 3 (LL3) female larvae were placed into new vials with fresh cornmeal food. When LL3 female larvae began metamorphosis, white pupae were placed into an empty vial and designated as being at 0h after pupal formation (APF). Samples remained at 18°C until 24h APF and then were transferred to 30°C to induce *esg-Gal4* expression. Flies were then dissected at 34 hours or 42 hours later, followed by immunofluorescence staining. Based on previous studies comparing pupal development at 18°C and 30°C to 25°C (*21*), the dissection times chosen roughly correspond to 48 APF and 64 APF at 25°C.

Knock Down of Notch signaling during pupal development

esg^{ts}>GFP (control) and *esg^{ts}>GFP UAS-Dl RNAi* (or *UAS-Notch RNAi or UAS-Notch^{DN}*) flies were cultured at 18^{o}C. Late Larval 3 (LL3) female larvae were placed into new vials with fresh cornmeal food. When LL3 female larvae began metamorphosis, white pupae were placed into an empty vial and designated as being at 0h after pupal formation (APF). Samples remained at 18^{o}C until 24h APF and then were transferred to 30^{o}C to induce *esg-Gal4* expression. 65 hours later, which roughly corresponds to 92h APF at 25^{o}C, half of pupae were dissected and examined as described in the main text. Remaining pupae were kept at 30^{o}C and after eclosion (AE) were transferred to fresh cornmeal food vials accompanied by daily changes of food. At 3 days AE intestines were examined as described in the main text.

To determine when Notch signaling is required for preventing ISC differentiation into ee cells, *esg^{ts}>GFP UAS-Dl RNAi* and *esg^{ts}>GFP UAS-Notch RNAi* pupae were cultured at 18^{o}C until 86h APF (corresponds to 42h APF @ 25^{o}C), 110h APF (corresponds to 53h APF @ 25^{o}C), 133h APF (corresponds to 64h APF @ 25^{o}C), 157h APF (corresponds to 76h APF @ 25^{o}C) and 181h APF (corresponds to 87h APF @ 25^{o}C). Then pupae were transferred to 30^{o}C to permit *esg-Gal4* expression. Dissections were performed before eclosion, based on the appearance of black wings and mature bristles (*21*).

Notch, Delta and Bazooka mutant MARCM clone analysis during the pupal period

FRT19A MARCM Notch^{55e11}, *FRT19A MARCM baz^{4}*, FRT *19A* MARCM, 82B *MARCM*, and *FRT82B MARCM Dl^{RevF10}* flies were cultured in a 25^{o}C incubator. LL3 female larvae were placed into new vials with fresh cornmeal food. When LL3 female larvae began metamorphosis, white pupae were placed into an empty vial at 25^{o}C and designated as being at 0h after pupal

formation (APF). Pupae were heat shocked for 1 hour at 24h APF, and then moved back to 25°C. *FRT19A MARCM Notch*^{55e11}, FRT *19A* MARCM, 82B *MARCM*, and *FRT82B MARCM Dl*^{RevF10} intestines were dissected at 92h APF, 3 days AE, 5 days AE, and 10 days AE, followed by immunofluorescence staining. *FRT 19A* MARCM (control) and *FRT19A* MARCM *baz*^{4} intestines were dissected at 92h APF, followed by immunofluorescence staining. Adult flies were reared on cornmeal food that was changed daily.

Missexpression of Notch intracellular domains in ISCs during pupal development

esg^{ts}*>GFP*, *esg*^{ts}*>GFP UAS-Notch*^{intra1790}, *esg*^{ts}*>GFP UAS-Notch*$^{intra1792-2156}$, and *esg*^{ts}*>GFP UAS-Notch*$^{intra1895-2116}$ flies were cultured at 18°C incubator. When LL3 female larvae began metamorphosis, white pupae were placed into an empty vial at 18°C and designated as being at 0h after pupal formation (APF). Vials were kept at 18°C until 48h APF. *esg*^{ts}*>GFP* vials were placed at 30°C. *esg*^{ts}*>GFP UAS-Notch*^{intra1790} vials were placed either at 30°C, 27°C, 25°C, or 18°C. *esg*^{ts}*>GFP UAS-Notch*$^{intra1792-2156}$ and *esg*^{ts}*>GFP UAS-Notch*$^{intra1895-2116}$ flies were placed at 30°C. For all vials transferred to 30°C, dissections were performed before eclosion, based on the appearance of black wings and mature bristles (*21*), about 60 hours after temperature shift. *esg*^{ts}*>GFP UAS-Notch*^{inra1790} vials were transferred to 27°C or 25°C, dissections were performed before eclosion, about 70 hours after temperature shift. *esg*^{ts}*>GFP UAS-Notch*^{intra1790} vials were kept at 18°C incubator during all of pupal development and dissections were performed about 190h APF.

Pdm1 antibody production

Residues 95-226 of Pdm1 protein fragment (*47*) was cloned into the protein expression vector pDEST17 (Invitrogen), and used to transform BL21A competent cells. 6×His-tagged protein was purified from lysate using Ni–nitrilotriacetic acid flow columns (QIAGEN) and was injected into

guinea pigs (Covance). Sera were collected over a period of 2 months and tested for specificity by Western blot analysis and *nub*[1] MARCM clones (Fig. S5I). We did however note that staining of adult ECs with this antibody does not reproducibly stain EC nuclei and is therefore not recommended as a probe for adult EC differentiation.

Immunostaining and fluorescence microscopy

Samples were dissected in 1XPBS, fixed in 4% formaldehyde for 1 hour. Primary antibodies were used at the following dilutions: mouse anti-Pros at 1:100 (MR1A; Developmental Studies Hybridoma Bank); chicken anti-GFP at 1:10,000 (Abcam, Cat #13970); rat anti-α-tubulin at 1:2,000 (Abd Serotec MCA78G); guinea pig anti-Delta at 1:4,000 (obtained from Marc Muskavitch, Boston College); rabbit anti-Miranda at 1:1000 (antigen: peptide 96C, from amino acid 96 to 118, A96C, obtained from Yuh Nung Jan, University of California School of Medicine, San Francisco)(*11*); rabbit anti-GST-Baz Nterm at 1:2000 (final bleed, obtained from Elisabeth Knust, Max-Planck-Institute of Molecular Cell biology and Genetics, Dresden) (*8*); rabbit anti-β-galactosidase at 1:10,000 (Cappel); mouse anti- β-galactosidase at 1:400 (Abcam, Ab1047) ; guinea pig anti-Pdm1 at 1:1,000; rabbit anti-DH31 at 1:1,000 (obtained from Gert Jan Veenstra, Nijmegen Centre for Molecular Life Sciences)(*48*); rabbit anti-FMRFamide at 1:1,000 (Peninsula Laboratories, Inc. Cat# T4321); mouse anti-Notch intracellular domain ($Notch^{intra}$) at 1:100 (C17.9C6; Developmental Studies Hybridoma Bank), and rabbit anti-phospho-histone H3 at 1:1000 (H3ser10, Millipore #2465253). Alexa Fluor–conjugated secondary antibodies were used at 1:4,000 (Molecular Probes and Invitrogen). Guts were stained with 1 μg/ml DAPI (Sigma-Aldrich), mounted in 70% glycerol, and imaged with a spinning-disc confocal microscope (DSU; Olympus) using UPLFLN 20×, 40× oil, and 60× oil objectives (imaging

medium: immersion oil type F obtained from Olympus). The imaging temperature was at room temperature. The camera used was an electron multiplying charge-coupled device camera (ImagEM Enhanced C9100-13; Hamamatsu Photonics). The acquisition and processing software used was SlideBook (version 4.2; Intelligent Imaging Innovations). Images were processed in Photoshop CS5 (Abode) and Illustrator CS4 (Adobe) for image merging and resizing.

Quantification of Notch^{intra} fluorescence integrated density

esg^{ts}>GFP+Notch^{inra1790} female pupae were cultured at 18^{o}C until 48h APF and then shifted to 30^{o}C, 27^{o}C and 25^{o}C respectively for 16 hours. Intestines were immediately dissected followed by Notch^{intra} antibody staining. Notch^{intra} fluorescence pictures were taken at the same microscopy settings and then processed using imageJ to quantify fluorescence-integrated density.

2-cell *WT MARCM* clones induction during the adult period

FRT82B MARCM flies were cultured at 25^{o}C. 5 days AE, flies were heat shocked for 45 minutes. 2 days ACI, intestines were examined by immunofluorescence staining.

Missexpression of Asense and Notch RNAi during the adult period

esg^{ts}>GFP UAS-Asense and *esg^{ts}>GFP UAS-Asense UAS-Notch RNAi* flies were cultured in a 18^{o}C incubator. 5 days AE, flies were transferred to a 30^{o}C incubator. 36 hours after temperature shift, *esg^{ts}>GFP UAS-Asense* intestines were examined for Pros asymmetric localization. 3 days after temperature shift, *esg^{ts}>GFP UAS-Asense* intestines were examined for Dl and *NRE-lacZ* staining. 8 days after temperature shift, *esg^{ts}>GFP UAS-Asense* and *esg^{ts}>GFP UAS-Asense UAS-Notch RNAi* intestines were examined for ISC loss.

Missexpression of Asense in WT and Dl mutant MARCM clones during the adult period

UAS-Asense; *FRT82B MARCM* flies and *UAS-Asense*; *FRT82B* Dl^{RevF10} *MARCM* flies were reared in a 25^{o}C incubator. 3 days AE, flies were heat shocked for 45 minutes. 5 days and 10 days ACI, intestines were examined followed by immunofluorescence staining.

Statistical analysis and Graphing

Boxes in Fig. 5F and S8J extend from the 25th to 75th percentiles. Whiskers extend to the 10 to 90 percentiles. Statistics were performed using one-way analysis of variance (ANOVA) test on Prism (GraphPad Software). Significance was accepted at *, $P < 0.01$; **, $P < 0.001$; and ***, $P < 0.0001$. Radial histogram graph is made by using OriginPro 8.5.1. (OriginLabs).

Figures S1-S10

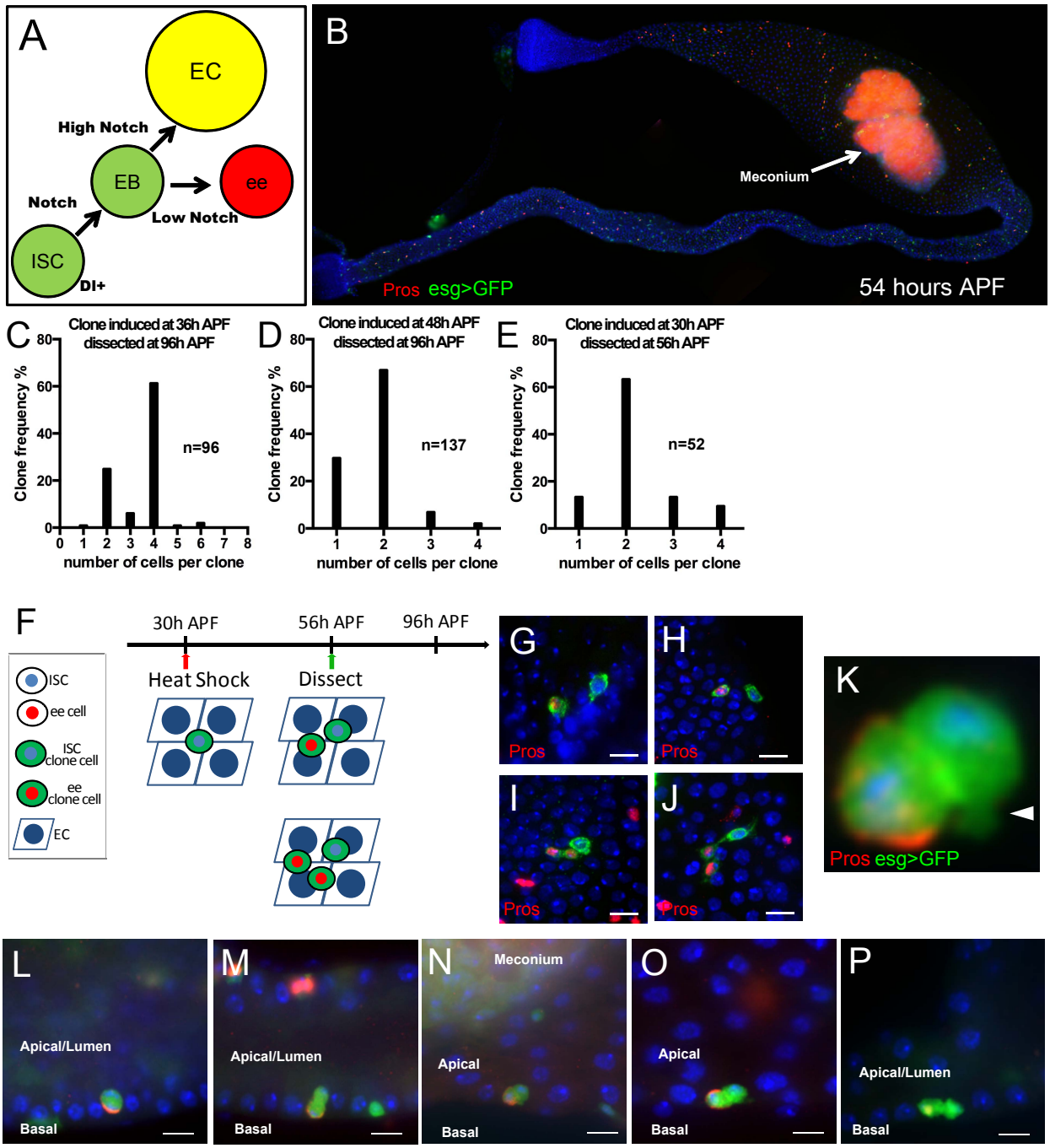

Sup Fig. 1. ee cells are specified by ISC asymmetric divisions. (A) Previous model of the *Drosophila* intestinal stem cell (ISC) lineage: ISCs express Delta and signal via the Notch signaling pathway to their daughter, the enteroblast (EB), to differentiate into an EC or an ee cell. An EB that receives a high Notch signal differentiates into an EC. An EB that receives a low Notch signal differentiates into an ee. (B) At 54h APF, Pros is present in the entire intestine. (C) Quantification of the frequency of different size clones induced at 36h APF and examined at 96h APF. Clones counted: n=96. (D) Quantification of the frequency of different size clones induced at 48h APF and examined at 96h APF. Clones counted: n=137. (E) Quantification of the frequency of different size clones induced at 30h APF and examined at 56h APF. Clones

counted: n=52. (F) Schematic representation of *WT* MARCM clones and their outcomes induced at 30h APF and examined at 56h APF. (G and H) 2-cell clones (green) induced at 30h APF contain 1 Pros+ cell and 1 Pros- cell. (I and J) 3-cell clones induced at 30h APF contain 2 Pros+ cells and 1 Pros- cell. (K) High magnification image of Fig. 1L. The apical daughter extends a projection (arrowhead) towards the basal side during telophase. (L-P) Low magnification images of Fig. 1J-N respectively. Pros asymmetrically localizes to the basal daughter cell during ISC mitosis. Blue: DAPI. Green in J-O: *esg>GFP*. Scale bar: 10μm.

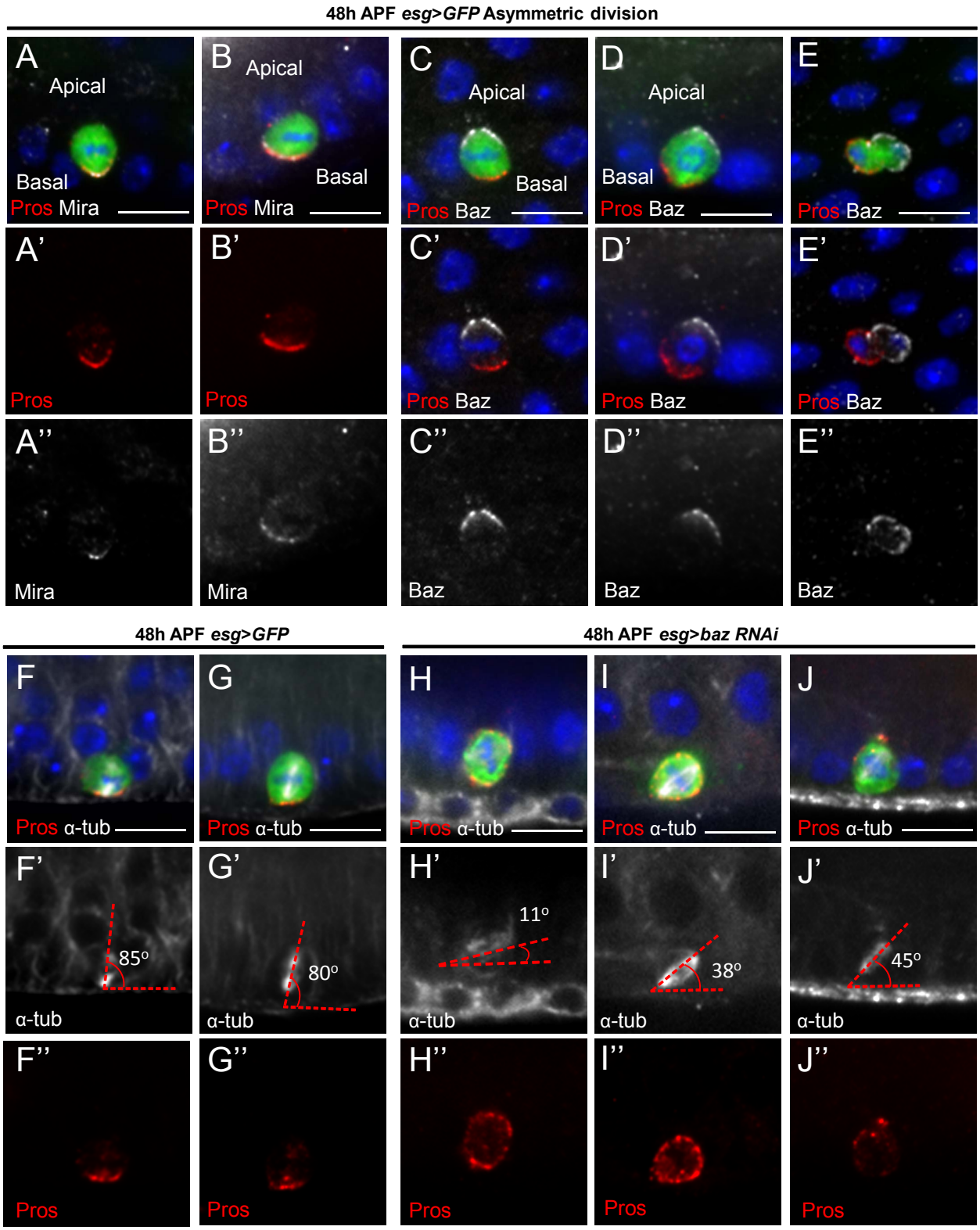

Sup Fig. 2. Baz is required for the asymmetric localization of Prospero during ISC mitosis. (A-J) Pupal midguts were examined at 48h APF. (A and B) Mira co-localizes with Pros on the basal side of metaphase ISCs. White: Mira. (C, D and E) Crescent Baz and Pros staining are mutually exclusive in (C) metaphase and (D) anaphase and (E) Telophase ISCs. White: Baz. (F

and G) Representative division angles in *esg>GFP* metaphase ISCs. Pros staining localizes to the basal side of dividing cells. White: α-tub. (H, I and J) Representative division angles in *esg*^{ts}*>baz RNAi* metaphase ISCs. Pros evenly distributes on the cell membrane. Red: Pros. Blue: DAPI. Scale bars: 10μm.

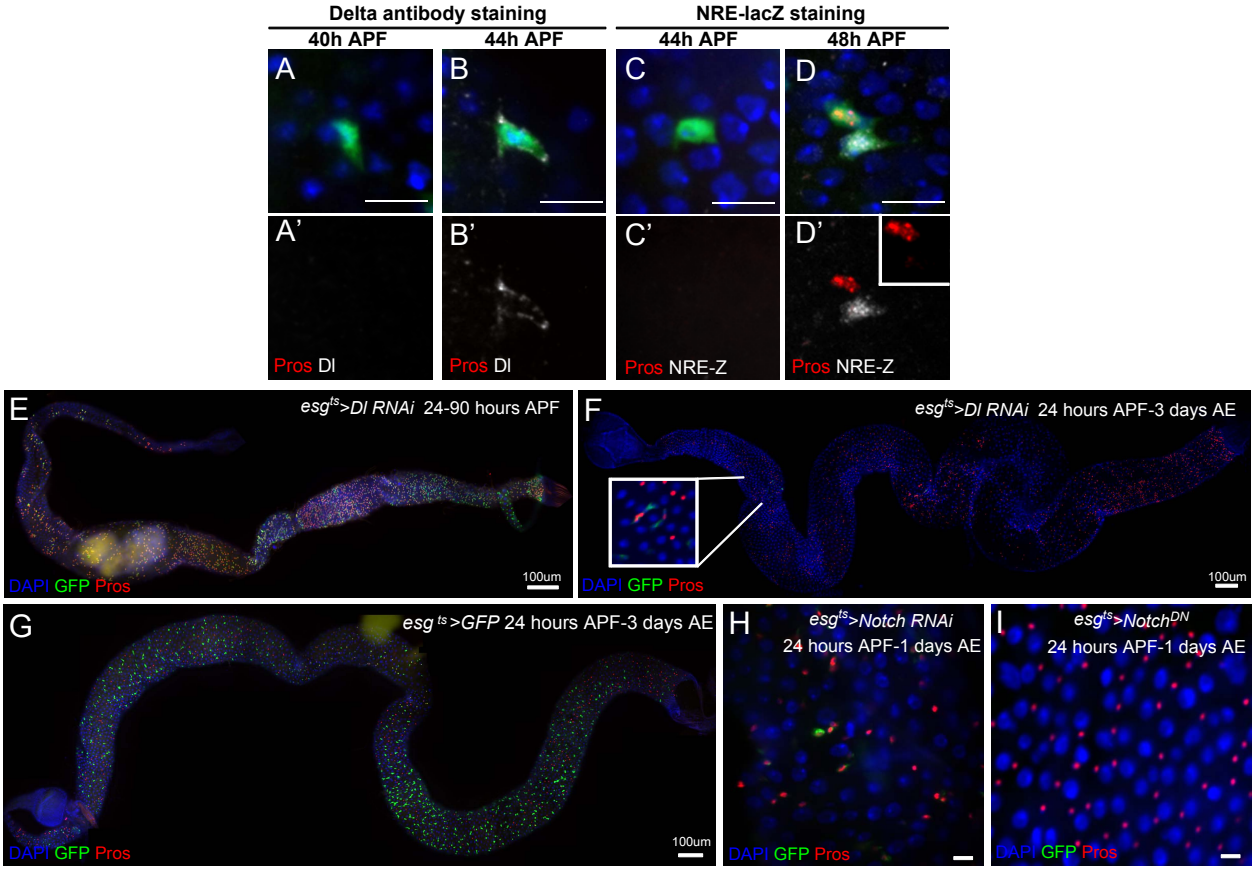

Sup Fig. 3. ee cells activate Notch signaling in ISCs to prevent ISCs from differentiating into ee cells during pupal development. (A, A') Dl is absent from *esg>GFP*+ ISCs at 40h APF. (B, B') Membrane punctate Dl is present in *esg>GFP*+ ISCs at 44h APF. (C, C') *NRE-lacZ* staining is absent from a single *esg>GFP*+ ISC at 44h APF. (D, D') An ISC-ee pair of cells at 48h APF. *NRE-lacZ* is present in the Pros- *esg>GFP*+ ISC at 48h APF. Insert in D': Pros. (E-I) Flies were transferred to 30^{o}C at 24h APF. (E) At 90h APF all *esg*^{ts}*>Dl RNAi*, GFP+ cells are Pros+. (F) At 3 days AE, rare GFP positive cells are present in *esg*^{ts}*>Dl RNAi* GFP intestine. All remaining diploid cells (GFP-) are Pros+. Insert: rare GFP+ cells. (G) *esg*^{ts}*>GFP* control intestines were dissected at 3 days AE. *esg*^{ts}*>GFP* labels all ISCs and EBs. (H) *esg*^{ts}*>Notch RNAi* flies or (I) *esg*^{ts}*>Notch*^{DN} flies were dissected at 1 day AE. Mutant midguts contain few or no *esg*^{ts}*>GFP* positive cells. All remaining diploid cells (GFP-) are Pros+. Blue: DAPI. Scale bar in A-D and H-I: 10μm.

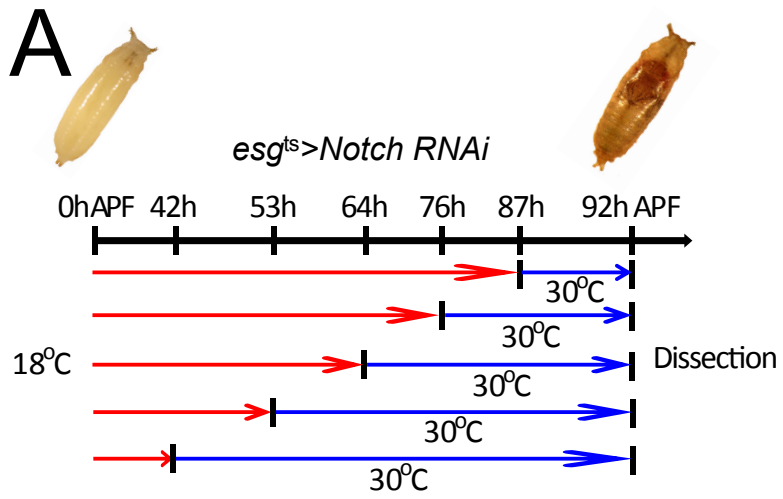
A
esg^ts>Notch RNAi
0hAPF 42h 53h 64h 76h 87h 92h APF
30°C
30°C
18°C
Dissection
30°C
30°C
30°C

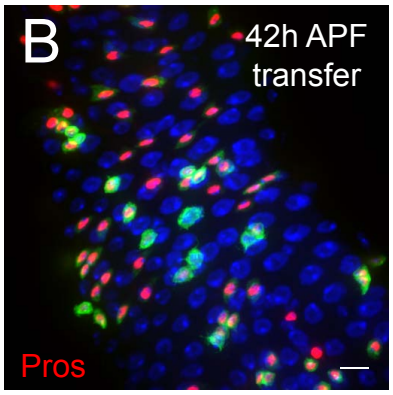
B
42h APF
transfer
Pros

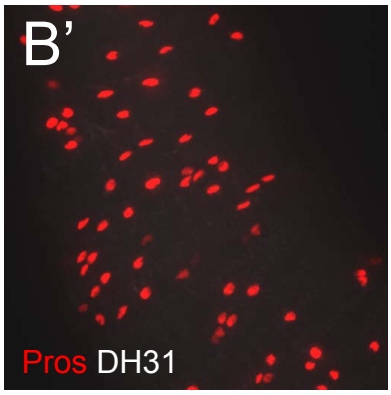
B'
Pros DH31

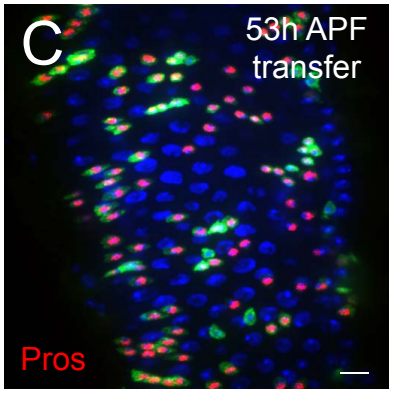
C
53h APF
transfer
Pros

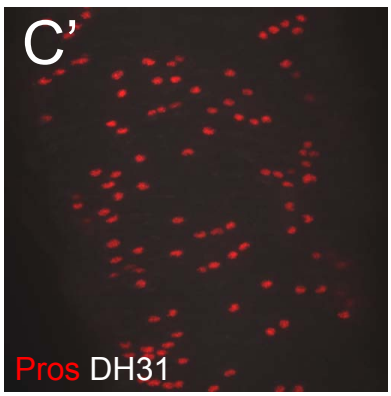
C'
Pros DH31

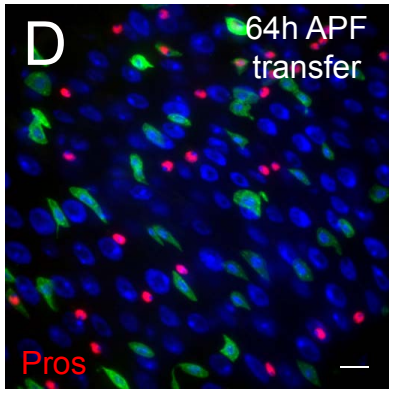
D
64h APF
transfer
Pros

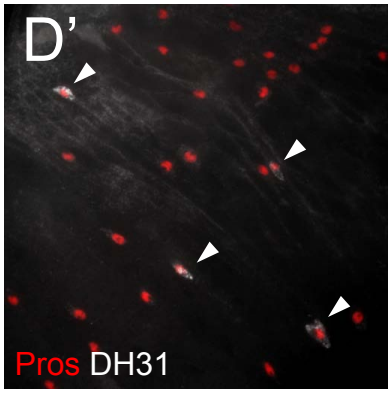
D'
Pros DH31

Sup Fig. 4. Notch signaling is dispensable for pupal ISC maintenance after 64h APF. Hours in this Figure correspond to developmental times at 25^{o}C (see Material and Methods for experiment details). (A) Schematic of the genetic manipulations carried out during pupal development. (B and B') 42h APF, *esg*^{ts}>*Notch RNAi* pupae were transferred to 30^{o}C. (C and C') 53h APF, *esg*^{ts}>*Notch RNAi* pupae were transferred to 30^{o}C. (B' and C') No Mira staining was detectable. (D and D') 64h APF, *esg*^{ts}>*Notch RNAi* pupae were transferred to 30^{o}C. Arrowhead in D': DH31 staining positive cells. Blue: DAPI. Red: Pros. White: DH31. Scale bar: 10μm.

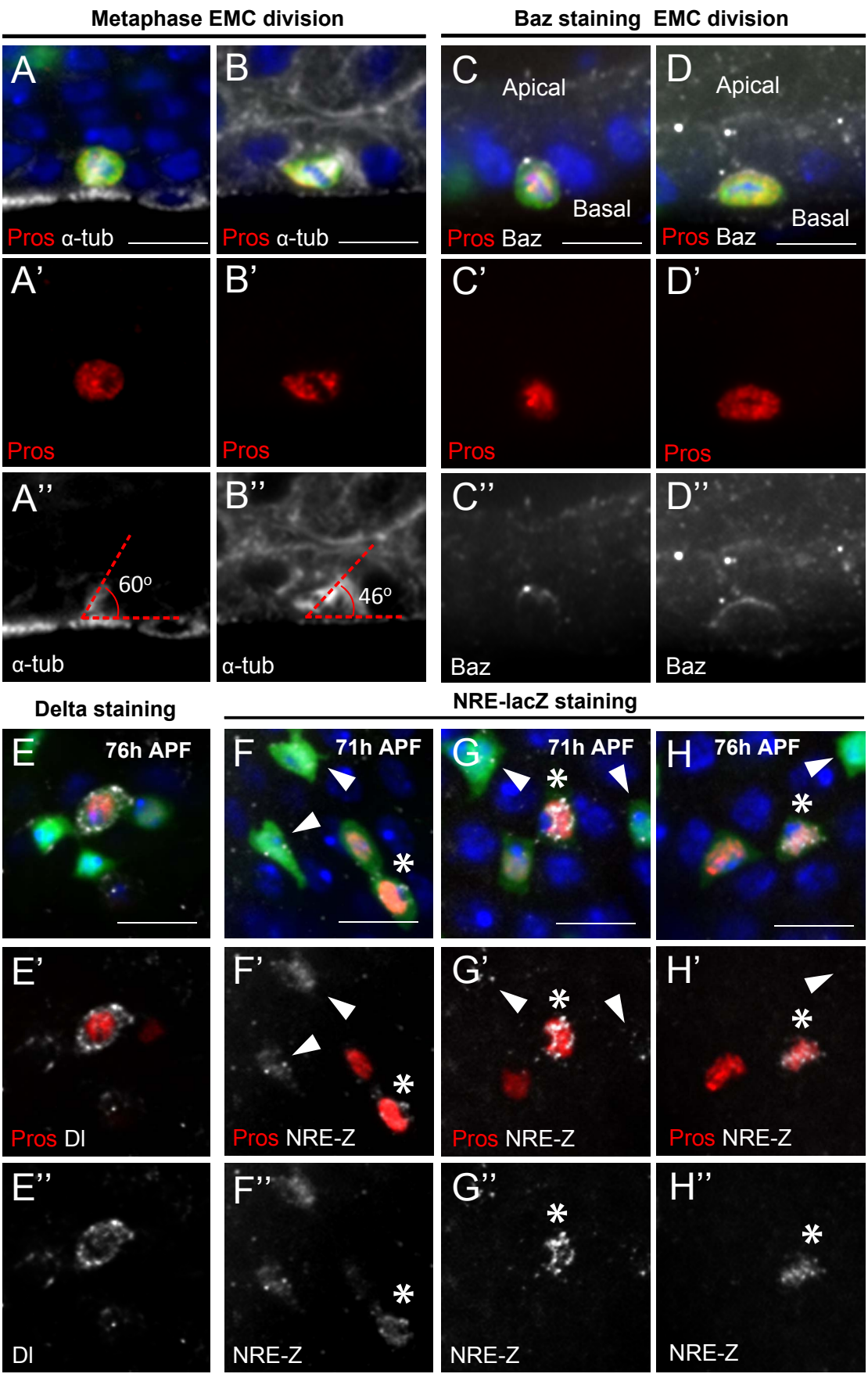
Metaphase EMC division
Baz staining EMC division
A
B
C
Apical
Basal
D
Apical
Basal
Pros α-tub
Pros α-tub
Pros Baz
Pros Baz
A'
B'
C'
D'
Pros
Pros
Pros
Pros
A''
B''
C''
D''
60°
46°
α-tub
α-tub
Baz
Baz
Delta staining
NRE-lacZ staining
E
76h APF
F
71h APF
G
71h APF
H
76h APF
E'
F'
G'
H'
Pros Dl
Pros NRE-Z
Pros NRE-Z
Pros NRE-Z
E''
F''
G''
H''
Dl
NRE-Z
NRE-Z
NRE-Z

Sup Fig. 5. ee cell divisions are symmetric for Prospero distribution but asymmetric for cell polarity and Notch signaling. (A-A'' and B-B'') Representative division angles in metaphase of ee cell divisions. (C-C'' and D-D'') Baz staining localizes to a crescent on the apical cell membrane during metaphase of ee divisions. (E-E'') Following ee division, strong Dl staining is present in one of the Pros+ pairs of cells. (F-F'', G-G'', and H-H'') After ee cell division, one of the two Pros+ cells is *NRE-lacZ* positive (asterisk). *NRE-lacZ* staining in ISCs (arrowheads in F, G and H) is dynamic. *NRE-lacZ* staining is present in (F), low in (G) and disappeared in (H). Blue: DAPI. Scale bar: 10μm.

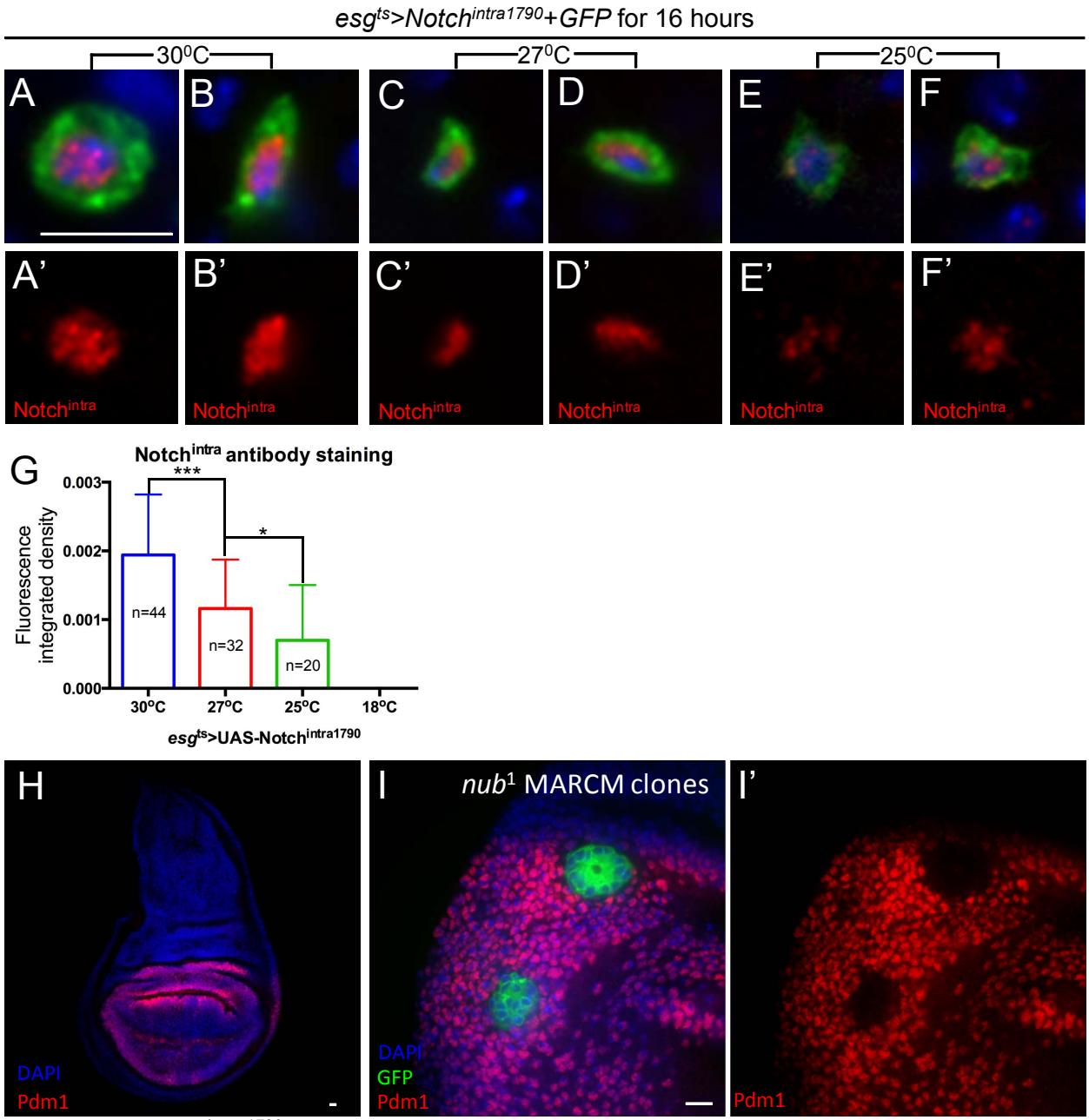

Sup Fig. 6. Notch^{intra1790} expression levels driven by *esg*^{ts} at different temperatures and specification of Pdm1 antibody. (A-F) *esg*^{ts}>*Notch*^{intra1790} flies were cultured at 18°C and

transferred to (A-A' and B-B') 30°C, (C-C' and D-D') 27°C, or (E-E' and F-F') 25°C at 48h APF for 16 hours. The expression level of Notch^{intra1790} was detected by Notch^{intra} antibody staining. Both Notch^{intra1790} and GFP staining appear weaker when the temperature is lower. (G) Quantification of the fluorescence integrated density of Notch^{intra} staining at different temperatures. Data are represented as mean ± SD. ***: P<0.0001, *: P<0.01. (H) Pdm1 antibody staining (red) in the imaginal wing disc. (I, I') Pdm1 antibody staining (red) is absent from *nub*^{1} MARCM clones (Green) induced in the wing disk. Blue: DAPI. Scale bar: 10μm.

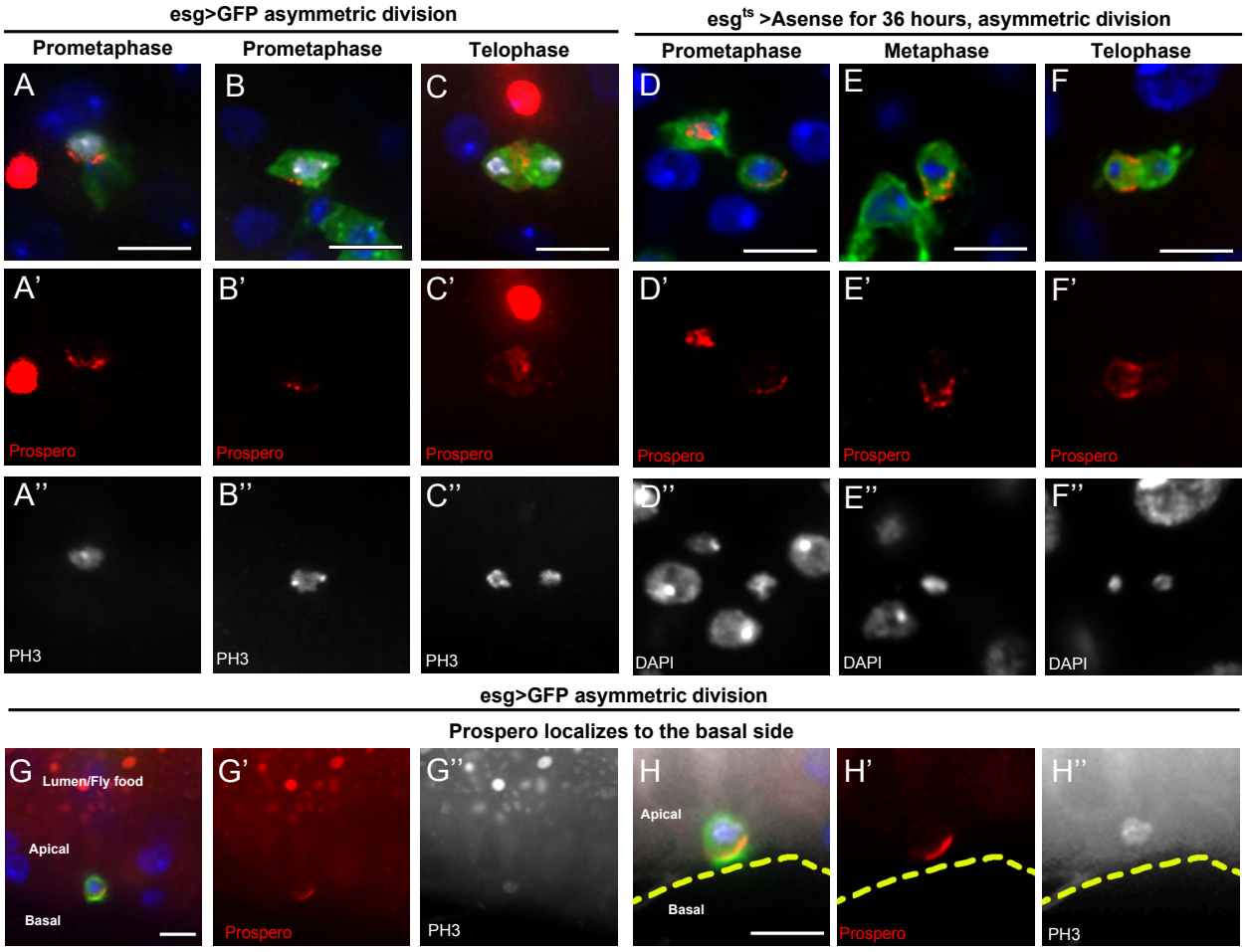

Sup Fig. 7. Pros asymmetrically localizes into the basal daughter cell during adult ISC divisions. (A-A'' and B-B'') Pros asymmetrically localizes to a crescent in dividing *esg>GFP+* cells in the adult. (C-C'') Pros asymmetrically localizes into one of the daughter cells during Telophase of adult ISC division. (D-D'', E-E'' and F-F'') 5 days AE *esg*^{ts}>Asense flies were transferred to 30°C for 36 hours. Pros asymmetrically localizes to a crescent in dividing *esg*^{ts}*>Asense, GFP+* cells. (G-G'') Low magnification of a dividing adult *esg>GFP+* cell containing Pros asymmetrically localized to the basal side. (H) High magnification of the cell in (G). The yellow line indicates location of the basement membrane. Blue: DAPI. Scale bar: 10μm.

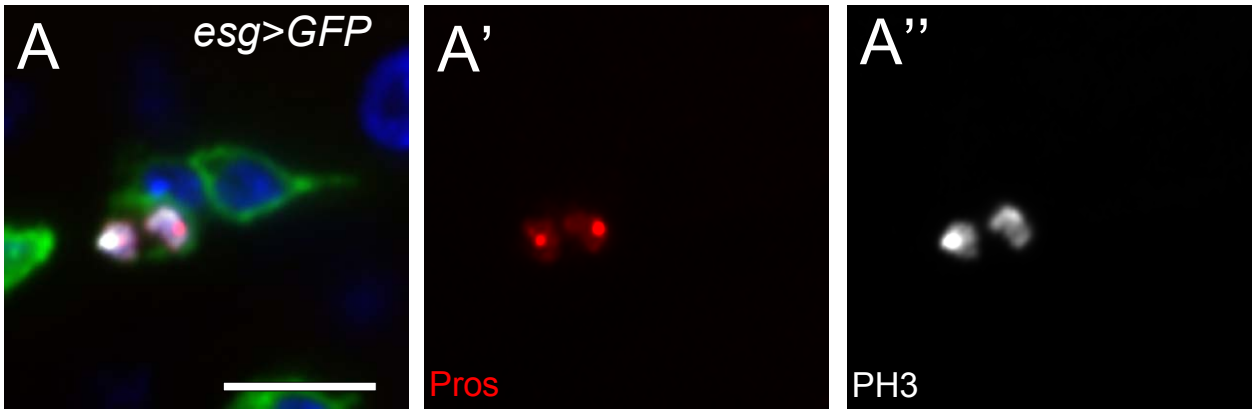

Sup Fig. 8. Symmetric localization of Pros during an ee division in the adult intestine. Blue: DAPI. Scale bar: 10μm.

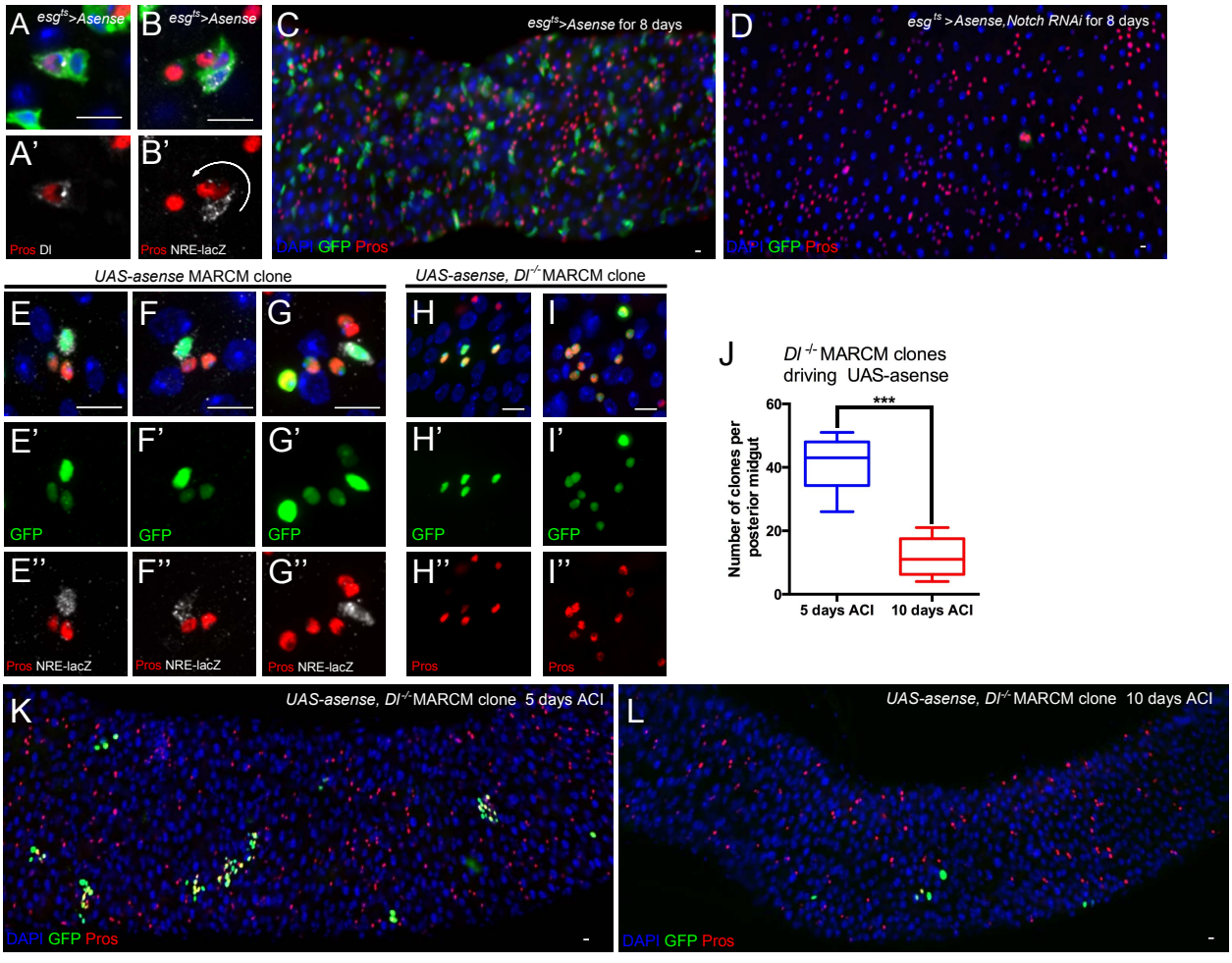

Sup Fig. 9. Post mitotic Notch signaling from enteroendocrine daughters regulates ISC identity. (A-A' and B-B') 5 days AE, *esg*^{ts}*>Asense* flies were transferred to 30^{o}C for 3 days. (A) Dl staining is present in the Pros+ cell from a pair of *esg>GFP*+ cells. (B) A four-cell *esg>GFP*+ cluster contains 3 ee cells (Nuclear Pros+) and a single ISC (Pros-) that is positive

for the Notch reporter *NRE-lacZ*. Note that the strongest GFP+ cell in the cluster is the ISC. The arrow in B' indicates the most likely division order in the lineage. (C) 3 days after eclosion *esg^{ts}>Asense* flies were transferred to 30^{o}C for 8 days. The intestine contains numerous clusters of enteroendocrine cells. ISCs (GFP+ and Pros-) are also present. (D) 3 days after eclosion *esg^{ts}>Asense, Notch RNAi* flies were transferred to 30^{o}C for 8 days. In contrast to (C), ISCs are no longer present. (E-E'', F-F'' and G-G'') *WT* MARCM clones expressing *UAS-asense* for 5 days After Clone Induction (ACI). Each of these clones contains one ISC (Pros-) that is also positive for the Notch reporter *NRE-lacZ*. (H-H'' and I-I'') *Dl^{RevF10}* MARCM clones expressing *UAS-asense* for 5 days ACI. All clone cells are Pros+. (H) is a lower magnification view of Fig. 6F. (J) Quantification of the number of *UAS-asense*; *Dl^{RevF10}* MARCM clones in the posterior midgut 5 days and 10 days ACI. ***: P<0.0001. (K) A low magnification view of *UAS-asense*; *Dl^{RevF10}* MARCM intestine 5 days ACI. (L) A low magnification view of *UAS-asense*; *Dl^{RevF10}* MARCM intestine10 days ACI. Blue: DAPI. Scale bar: 10μm.

A

Notch signaling in larval midgut

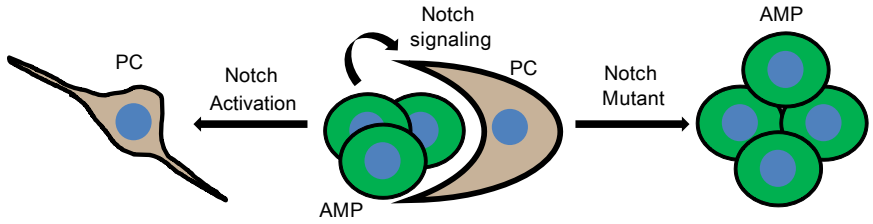

B

Notch signaling in pupal midgut

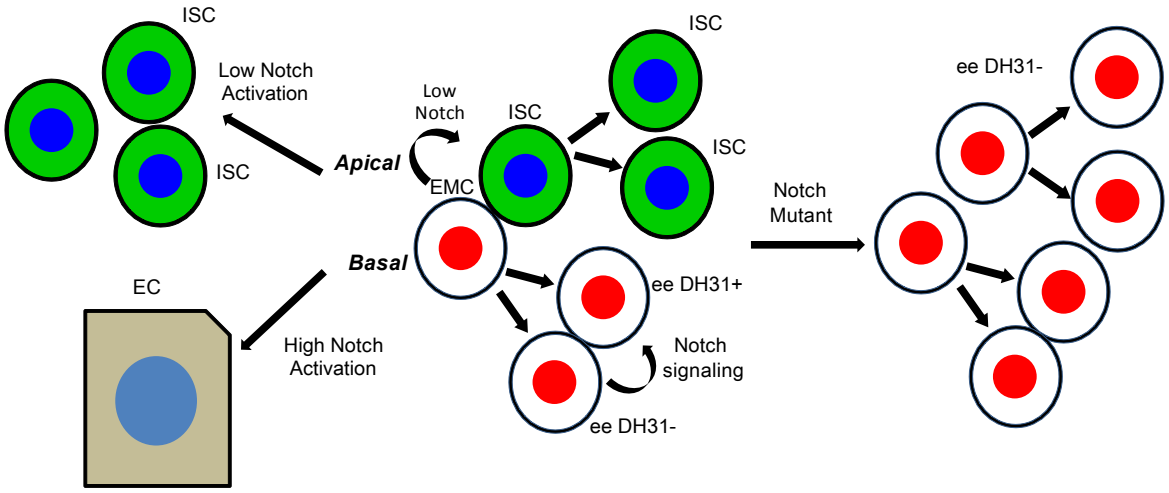

C

Notch signaling in adult midgut

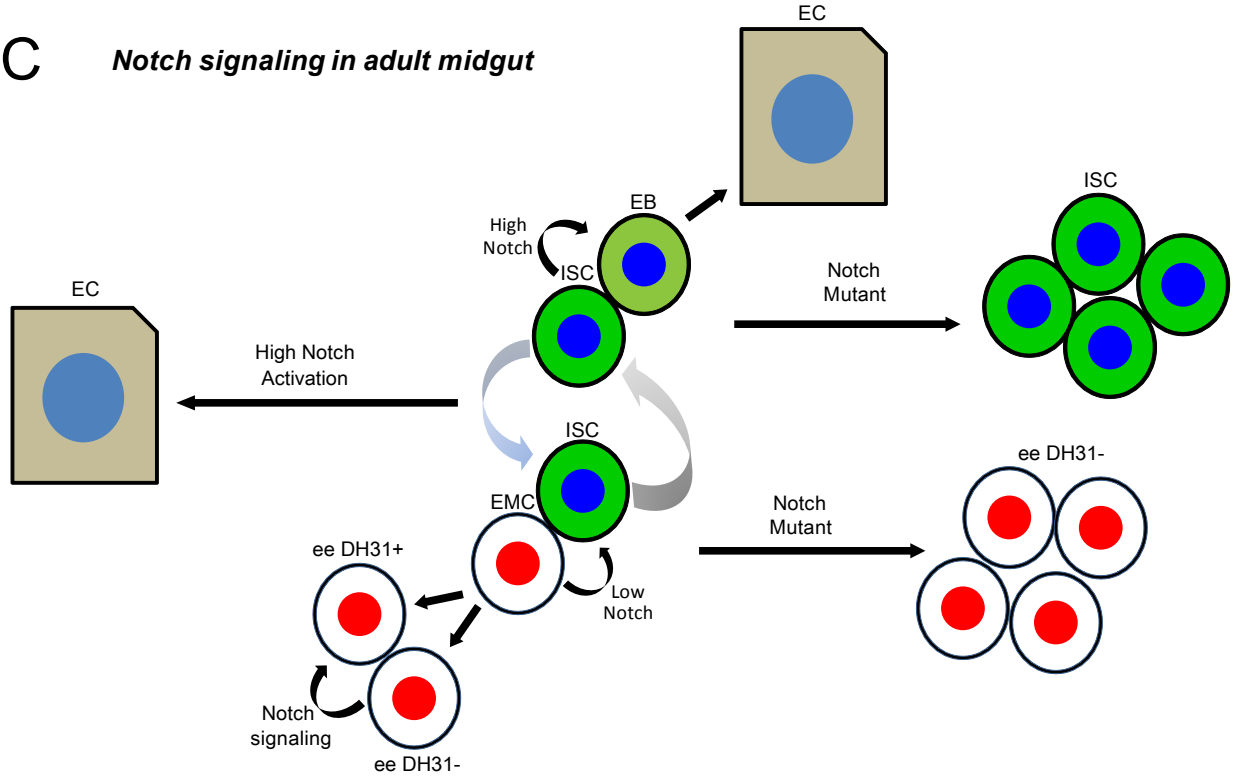

Sup Fig. 10. Model of Notch function in the larval, pupal and adult midgut. (A) Larval midgut. Notch signaling is necessary and sufficient for Peripheral Cell differentiation (PC) from Adult Midgut Progenitors (AMPs). (B) Pupal midgut. Following asymmetric division of ISCs, Enteroendocrine Mother Cell (EMC) daughters activate low Notch signaling in ISCs to prevent their differentiation into ee cells. After one round of asymmetric ISC divisions, ISCs divide symmetrically giving rise to a pair of ISCs. EMCs divide asymmetrically producing one Notch positive DH31+ ee cell and one Dl positive DH31- ee cell. Loss of Notch signaling during asymmetric ISC divisions results in ee cells that fail to express the peptide hormone DH31. Low level activation of Notch signaling in ISCs blocks ee cell formation. High level activation of Notch signaling in ISCs forces all ISCs to differentiate into ECs. (C) Adult midgut. ISCs strongly activate the Notch signaling pathway in enteroblast (EB) daughters resulting in their differentiation into ECs. Occasionally, ISCs express Pros and initiate the ee cell making process. Following asymmetric cell division, the EMC activates low Notch signaling in ISCs causing them to revert back to making ECs. In addition, EMCs undergo one transient division resulting in an ee cell pair, which requires Notch pathway activation to properly differentiate into hormone producing cells. Disruption of the Notch signaling pathway during the EC making process results in an accumulation of ISCs. Disruption of the Notch signaling during the ee making process results in an accumulation of ee cells. As a result mutant ISCs become unipotent and give rise to only ee cells. Activation of high level of Notch signaling promotes all adult ISCs to differentiate into ECs.

References

1. C. A. Micchelli, N. Perrimon, Evidence that stem cells reside in the adult *Drosophila* midgut epithelium. *Nature* **439**, 475–479 (2006). Medline doi:10.1038/nature04371

2. B. Ohlstein, A. Spradling, The adult *Drosophila* posterior midgut is maintained by pluripotent stem cells. *Nature* **439**, 470–474 (2006). Medline doi:10.1038/nature04333

3. B. Ohlstein, A. Spradling, Multipotent *Drosophila* intestinal stem cells specify daughter cell fates by differential notch signaling. *Science* **315**, 988–992 (2007). Medline doi:10.1126/science.1136606

4. C. A. Micchelli, L. Sudmeier, N. Perrimon, S. Tang, R. Beehler-Evans, Identification of adult midgut precursors in *Drosophila*. *Gene Expr. Patterns* **11**, 12–21 (2011). Medline doi:10.1016/j.gep.2010.08.005

5. S. Takashima, K. L. Adams, P. A. Ortiz, C. T. Ying, R. Moridzadeh, A. Younossi-Hartenstein, V. Hartenstein, Development of the *Drosophila* entero-endocrine lineage and its specification by the Notch signaling pathway. *Dev. Biol.* **353**, 161–172 (2011). Medline doi:10.1016/j.ydbio.2011.01.039

6. T. Lee, L. Luo, Mosaic analysis with a repressible cell marker (MARCM) for *Drosophila* neural development. *Trends Neurosci.* **24**, 251–254 (2001). Medline doi:10.1016/S0166-2236(00)01791-4

7. M. Schober, M. Schaefer, J. A. Knoblich, Bazooka recruits Inscuteable to orient asymmetric cell divisions in *Drosophila* neuroblasts. *Nature* **402**, 548–551 (1999). Medline doi:10.1038/990135

8. A. Wodarz, A. Ramrath, U. Kuchinke, E. Knust, Bazooka provides an apical cue for Inscuteable localization in *Drosophila* neuroblasts. *Nature* **402**, 544–547 (1999). Medline doi:10.1038/990128

9. Y. Izumi, N. Ohta, A. Itoh-Furuya, N. Fuse, F. Matsuzaki, Differential functions of G protein and Baz-aPKC signaling pathways in *Drosophila* neuroblast asymmetric division. *J. Cell Biol.* **164**, 729–738 (2004). Medline doi:10.1083/jcb.200309162

10. H. Ikeshima-Kataoka, J. B. Skeath, Y. Nabeshima, C. Q. Doe, F. Matsuzaki, Miranda directs Prospero to a daughter cell during *Drosophila* asymmetric divisions. *Nature* **390**, 625–629 (1997). Medline doi:10.1038/37641

11. C. P. Shen, L. Y. Jan, Y. N. Jan, Miranda is required for the asymmetric localization of Prospero during mitosis in *Drosophila*. *Cell* **90**, 449–458 (1997). Medline doi:10.1016/S0092-8674(00)80505-X

12. J. Hirata, H. Nakagoshi, Y. Nabeshima, F. Matsuzaki, Asymmetric segregation of the homeodomain protein Prospero during *Drosophila* development. *Nature* **377**, 627–630 (1995). Medline doi:10.1038/377627a0

13. J. A. Knoblich, L. Y. Jan, Y. N. Jan, Asymmetric segregation of Numb and Prospero during cell division. *Nature* **377**, 624–627 (1995). Medline doi:10.1038/377624a0

14. E. P. Spana, C. Q. Doe, The prospero transcription factor is asymmetrically localized to the cell cortex during neuroblast mitosis in *Drosophila*. *Development* **121**, 3187–3195 (1995). Medline

15. S. Fuerstenberg, C. Y. Peng, P. Alvarez-Ortiz, T. Hor, C. Q. Doe, Identification of Miranda protein domains regulating asymmetric cortical localization, cargo binding, and cortical release. *Mol. Cell. Neurosci.* **12**, 325–339 (1998). Medline doi:10.1006/mcne.1998.0724

16. F. Matsuzaki, T. Ohshiro, H. Ikeshima-Kataoka, H. Izumi, miranda localizes staufen and prospero asymmetrically in mitotic neuroblasts and epithelial cells in early *Drosophila* embryogenesis. *Development* **125**, 4089–4098 (1998). Medline

17. A. J. Schuldt, J. H. Adams, C. M. Davidson, D. R. Micklem, J. Haseloff, D. St Johnston, A. H. Brand, Miranda mediates asymmetric protein and RNA localization in the developing nervous system. *Genes Dev.* **12**, 1847–1857 (1998). Medline doi:10.1101/gad.12.12.1847

18. C. P. Shen, J. A. Knoblich, Y. M. Chan, M. M. Jiang, L. Y. Jan, Y. N. Jan, Miranda as a multidomain adapter linking apically localized Inscuteable and basally localized Staufen and Prospero during asymmetric cell division in *Drosophila*. *Genes Dev.* **12**, 1837–1846 (1998). Medline doi:10.1101/gad.12.12.1837

19. F. Roegiers, Y. N. Jan, Asymmetric cell division. *Curr. Opin. Cell Biol.* **16**, 195–205 (2004). Medline doi:10.1016/j.ceb.2004.02.010

20. V. Zecchini, K. Brennan, A. Martinez-Arias, An activity of Notch regulates JNK signalling and affects dorsal closure in *Drosophila*. *Curr. Biol.* **9**, 460 (1999).

21. S. P. Bainbridge, M. Bownes, Staging the metamorphosis of *Drosophila melanogaster*. *J. Embryol. Exp. Morphol.* **66**, 57–80 (1981). Medline

22. W. C. Lee, K. Beebe, L. Sudmeier, C. A. Micchelli, Adenomatous polyposis coli regulates *Drosophila* intestinal stem cell proliferation. *Development* **136**, 2255–2264 (2009). Medline doi:10.1242/dev.035196

23. M. P. Zeidler, C. Tan, Y. Bellaiche, S. Cherry, S. Häder, U. Gayko, N. Perrimon, Temperature-sensitive control of protein activity by conditionally splicing inteins. *Nat. Biotechnol.* **22**, 871–876 (2004). Medline doi:10.1038/nbt979

24. S. Kidd, T. Lieber, M. W. Young, Ligand-induced cleavage and regulation of nuclear entry of Notch in *Drosophila melanogaster* embryos. *Genes Dev.* **12**, 3728–3740 (1998). Medline doi:10.1101/gad.12.23.3728

25. B. Biteau, H. Jasper, Slit/Robo signaling regulates cell fate decisions in the intestinal stem cell lineage of *Drosophila*. *Cell Rep.* **7**, 1867–1875 (2014). Medline doi:10.1016/j.celrep.2014.05.024

26. N. Zielke, J. Korzelius, M. van Straaten, K. Bender, G. F. Schuhknecht, D. Dutta, J. Xiang, B. A. Edgar, Fly-FUCCI: A versatile tool for studying cell proliferation in complex tissues. *Cell Rep.* **7**, 588–598 (2014). Medline doi:10.1016/j.celrep.2014.03.020

27. X. Zeng, S. X. Hou, Enteroendocrine cells are generated from stem cells through a distinct progenitor in the adult *Drosophila* posterior midgut. *Development* **142**, 644–653 (2015). Medline doi:10.1242/dev.113357

28. A. J. Bardin, C. N. Perdigoto, T. D. Southall, A. H. Brand, F. Schweisguth, Transcriptional control of stem cell maintenance in the *Drosophila* intestine. *Development* **137**, 705–714 (2010). Medline doi:10.1242/dev.039404

29. X. Zeng, X. Lin, S. X. Hou, The Osa-containing SWI/SNF chromatin-remodeling complex regulates stem cell commitment in the adult *Drosophila* intestine. *Development* **140**, 3532–3540 (2013). Medline doi:10.1242/dev.096891

30. S. Goulas, R. Conder, J. A. Knoblich, The Par complex and integrins direct asymmetric cell division in adult intestinal stem cells. *Cell Stem Cell* **11**, 529–540 (2012). Medline doi:10.1016/j.stem.2012.06.017

31. C. Montagne, M. Gonzalez-Gaitan, Sara endosomes and the asymmetric division of intestinal stem cells. *Development* **141**, 2014–2023 (2014). Medline doi:10.1242/dev.104240

32. G. Emery, A. Hutterer, D. Berdnik, B. Mayer, F. Wirtz-Peitz, M. G. Gaitan, J. A. Knoblich, Asymmetric Rab 11 endosomes regulate delta recycling and specify cell fate in the *Drosophila* nervous system. *Cell* **122**, 763–773 (2005). Medline doi:10.1016/j.cell.2005.08.017

33. A. Rajan, A. C. Tien, C. M. Haueter, K. L. Schulze, H. J. Bellen, The Arp2/3 complex and WASp are required for apical trafficking of Delta into microvilli during cell fate specification of sensory organ precursors. *Nat. Cell Biol.* **11**, 815–824 (2009). Medline doi:10.1038/ncb1888

34. X. Zeng, L. Han, S. R. Singh, H. Liu, R. A. Neumüller, D. Yan, Y. Hu, Y. Liu, W. Liu, X. Lin, S. X. Hou, Genome-wide RNAi screen identifies networks involved in intestinal stem cell regulation in *Drosophila*. *Cell Rep.* **10**, 1226–1238 (2015). Medline doi:10.1016/j.celrep.2015.01.051

35. H. Nakagoshi, Functional specification in the *Drosophila* endoderm. *Dev. Growth Differ.* **47**, 383–392 (2005). Medline doi:10.1111/j.1440-169X.2005.00811.x

36. S. Artavanis-Tsakonas, C. Delidakis, R. G. Fehon, The Notch locus and the cell biology of neuroblast segregation. *Annu. Rev. Cell Biol.* **7**, 427–452 (1991). Medline doi:10.1146/annurev.cb.07.110191.002235

37. C. C. Homem, J. A. Knoblich, *Drosophila* neuroblasts: A model for stem cell biology. *Development* **139**, 4297–4310 (2012). Medline doi:10.1242/dev.080515

38. H. Wang, G. W. Somers, A. Bashirullah, U. Heberlein, F. Yu, W. Chia, Aurora-A acts as a tumor suppressor and regulates self-renewal of *Drosophila* neuroblasts. *Genes Dev.* **20**, 3453–3463 (2006). Medline doi:10.1101/gad.1487506

39. U. Koch, R. Lehal, F. Radtke, Stem cells living with a Notch. *Development* **140**, 689–704 (2013). Medline doi:10.1242/dev.080614

40. S. Fre, M. Huyghe, P. Mourikis, S. Robine, D. Louvard, S. Artavanis-Tsakonas, Notch signals control the fate of immature progenitor cells in the intestine. *Nature* **435**, 964–968 (2005). Medline doi:10.1038/nature03589

41. B. Z. Stanger, R. Datar, L. C. Murtaugh, D. A. Melton, Direct regulation of intestinal fate by Notch. *Proc. Natl. Acad. Sci. U.S.A.* **102**, 12443–12448 (2005). Medline doi:10.1073/pnas.0505690102

42. J. H. van Es, M. E. van Gijn, O. Riccio, M. van den Born, M. Vooijs, H. Begthel, M. Cozijnsen, S. Robine, D. J. Winton, F. Radtke, H. Clevers, Notch/gamma-secretase inhibition turns proliferative cells in intestinal crypts and adenomas into goblet cells. *Nature* **435**, 959–963 (2005). Medline doi:10.1038/nature03659

43. K. L. VanDussen, A. J. Carulli, T. M. Keeley, S. R. Patel, B. J. Puthoff, S. T. Magness, I. T. Tran, I. Maillard, C. Siebel, Å. Kolterud, A. S. Grosse, D. L. Gumucio, S. A. Ernst, Y. H. Tsai, P. J. Dempsey, L. C. Samuelson, Notch signaling modulates proliferation and differentiation of intestinal crypt base columnar stem cells. *Development* **139**, 488–497 (2012). Medline doi:10.1242/dev.070763

44. F. Radtke, H. R. MacDonald, F. Tacchini-Cottier, Regulation of innate and adaptive immunity by Notch. *Nat. Rev. Immunol.* **13**, 427–437 (2013). Medline doi:10.1038/nri3445

45. M. Mori, J. E. Mahoney, M. R. Stupnikov, J. R. Paez-Cortez, A. D. Szymaniak, X. Varelas, D. B. Herrick, J. Schwob, H. Zhang, W. V. Cardoso, Notch3-Jagged signaling controls the pool of undifferentiated airway progenitors. *Development* **142**, 258–267 (2015). Medline doi:10.1242/dev.116855

46. Z. Guo, I. Driver, B. Ohlstein, Injury-induced BMP signaling negatively regulates *Drosophila* midgut homeostasis. *J. Cell Biol.* **201**, 945–961 (2013). Medline doi:10.1083/jcb.201302049

47. S. L. Yeo, A. Lloyd, K. Kozak, A. Dinh, T. Dick, X. Yang, S. Sakonju, W. Chia, On the functional overlap between two *Drosophila* POU homeo domain genes and the cell fate specification of a CNS neural precursor. *Genes Dev.* **9**, 1223–1236 (1995). Medline doi:10.1101/gad.9.10.1223

48. J. A. Veenstra, H. J. Agricola, A. Sellami, Regulatory peptides in fruit fly midgut. *Cell Tissue Res.* **334**, 499–516 (2008). Medline doi:10.1007/s00441-008-0708-3